# Experimental demonstration of reduced tilt-to-length coupling by a two-lens imaging system

**Sönke Schuster,**[1,*] **Michael Tröbs,**[1] **Gudrun Wanner,**[1] **and Gerhard Heinzel**[1,2]

[1]*Max Planck Institute for Gravitational Physics (Albert Einstein Institute) and Institute for Gravitational Physics of the Leibniz Universität Hannover, Callinstr. 38, D-30167 Hannover, Germany*
[2]*gerhard.heinzel@aei.mpg.de*
[*]*soenke.schuster@aei.mpg.de*

**Abstract:**    The coupling between beam tilt and longitudinal path length readout in a setup representing a LISA test mass interferometer was reduced to below $2\,\mu$m/rad using a two lens imaging system. This was achieved by the use of a homodyne equal arm-length Mach-Zehnder interferometer and suppression of the dominating effects of higher order Gaussian modes and longitudinal actuator movement. The latter was subtracted using the phase signal of a large single element photo diode.

## References and links

1. K. Danzmann, A. Rdiger, R. Schilling, W. Winkler, and J. Hough, "LISA (laser interferometer space antenna), Proposal for a laser-interferometer gravitational wave detector in space," Report MPQ-177 (1993).
2. O Jennrich, "LISA technology and instrumentation," Class. Quantum Grav. **26**(15), 153001 (2009).
3. K. Danzmann, T. A. Prince, and the LISA international science team, "LISA assessment study report," European Space Agency ESA/SRE(2011), 3 (2011).
4. G. D. Racca and P. W. McNamara, "The LISA Pathfinder mission," Space Sci. Rev. **151**, 159–181 (2010).
5. F. Antonucci, M. Armano, H. Audley, G. Auger, M. Benedetti, P. Binetruy, C. Boatella, J. Bogenstahl, D. Bortoluzzi, P. Bosetti, M. Caleno, A. Cavalleri, M. Cesa, M. Chmeissani, G. Ciani, A. Conchillo, G. Congedo, I. Cristofolini, M. Cruise, K. Danzmann, F. De Marchi, M. Diaz-Aguilo, I. Diepholz, G. Dixon, R. Dolesi, N. Dunbar, J. Fauste, L. Ferraioli, D. Fertin, W. Fichter, E. Fitzsimons, M. Freschi, A. Garcia Marin, C. Garcia Marirrodriga, R. Gerndt, L. Gesa, F. Gilbert, D. Giardini, C. Grimani, A. Grynagier, B. Guillaume, F. Guzman, I. Harrison, G. Heinzel, M. Hewitson, D. Hollington, J. Hough, D. Hoyland, M. Hueller, J. Huesler, O. Jeannin, O. Jennrich, P. Jetzer, B. Johlander, C. Killow, X. Llamas, I. Lloro, A. Lobo, R. Maarschalkerweerd, S. Madden, D. Mance, I. Mateos, P. W. McNamara, J. Mendes, E. Mitchell, A. Monsky, D. Nicolini, D. Nicolodi, M. Nofrarias, F. Pedersen, M. Perreur-Lloyd, A. Perreca, E. Plagnol, P. Prat, G. D. Racca, B. Rais, J. Ramos-Castro, J. Reiche, J. A. Romera Perez, D. Robertson, H. Rozemeijer, J. Sanjuan, A. Schleicher, M. Schulte, D. Shaul, L. Stagnaro, S. Strandmoe, F. Steier, T. J. Sumner, A. Taylor, D. Texier, C. Trenkel, D. Tombolato, S. Vitale, G. Wanner, H. Ward, S. Waschke, P. Wass, W. J. Weber, and P. Zweifel. "LISA Pathfinder: mission and status," Classical Quan. Grav. **28**(9), 094001 (2011).
6. G Wanner, *Complex optical systems in space: Numerical modelling of the heterodyne interferometry of LISA Pathfinder and LISA,* (Dissertation at the Leibniz Universität of Hannover, 2010), Chap. 10, http://edok01.tib.uni-hannover.de/edoks/e01dh11/660137038.pdf
7. E. Morrison, B. J. Meers, D. I. Robertson, and H. Ward, "Automatic alignment of optical interferometers," Appl. Opt. **33**(22), 5041–5049 (1994).
8. E. Kochkina, G. Heinzel, G. Wanner, V. Mller, C. Mahrdt, B. Sheard, S. Schuster, and K. Danzmann, "Simulating and optimizing laser interferometers," ASP Conf. Ser. **467**, 291–292 (2012).

9.  G. Wanner, G. Heinzel, E. Kochkina, C. Mahrdt, B. Sheard, S. Schuster, and K. Danzmann, "Methods for simulating the readout of lengths and angles in laser interferometers with Gaussian beams," Opt. Commun. **285**(14), 4831–4839 (2012).
10. S. Schuster, G. Wanner, M. Trbs and G Heinzel. "Vanishing tilt-to-length coupling for a singular case in two-beam laser interferometers with Gaussian beams," Appl. Opt. **54**(5), 1010–1014 (2015).
11. B. Willke, N. Uehara, E. K. Gustafson, R. L. Byer, P. J. King, S. U. Seel, and R. L. Savage, "Spatial and temporal filtering of a 10-W Nd:YAG laser with a FabryPerot ring-cavity premode cleaner," Opt. Lett. **23**(21), 1704–1706 (1998).
12. D. Shaddock, M. Gray and D. McClelland, "Frequency locking a laser to an optical cavity by use of spatial mode interference," Opt. Lett. **24**(21), 1499–1501 (1999).
13. G. Heinzel, V. Wand, A. Garca, O. Jennrich, C. Braxmaier, D. Robertson, K. Middleton, D. Hoyland, A. Rdiger, R. Schilling, U. Johann, and K. Danzmann, "The LTP interferometer and phasemeter," Classical Quant. Grav. **21**(5), S581–S587 (2004).

---

## 1. Introduction

One significant noise source in high precision interferometric length measurements like LISA [1–3] or LISA Pathfinder [4, 5] is an unintended tilting (jittering) of the test mass. This angular jitter results in dithering beams, which in turn lead to noise in the path length readout. This effect is called tilt-to-length (TTL) coupling. In numerical simulations it was shown that it is possible to decrease TTL coupling by using imaging systems, which suppress the beam walk on the photo detectors [6]. However, the complete experimental verification of the predicted performance of such imaging optics proved to be complicated in previous attempts. The residual TTL coupling behind an imaging system due to other effects is much higher than the expected TTL coupling of an imaging system.

We list these noise sources (like non fundamental Gaussian beams, misalignment or detector noise), explain the mechanics that lead to additional TTL coupling and we show a laboratory experiment which reduces the number of noise sources, such that the noise reducing properties of an imaging system can be observed.

All investigations in this manuscript refer to the LISA mission [1–3] especially to the test mass interferometer. However, this type of imaging optics can be adapted to other interferometers.

## 2. Imaging systems in the test mass interferometer

Each LISA satellite follows the motion of two free-falling cubic blocks, called test mass(es) TM(s), one along each sensitive axis, inside the satellite which act as gravitational reference-sensors. The purpose of the TM interferometer is to measure the longitudinal movement of the TM as well as its tilt angles. A sketch of a TM interferometer is shown in Fig. 1. To suppress coupling between tilt angle and measurement of the longitudinal position the beam walk on the photo diode, originating from the tilt angle must be suppressed. For this purpose, two different types of imaging systems were considered in the past. The first is a classical pupil plane imaging system. It consists, due to the limited space on the LISA satellite, of at least four lenses. In an effort to reduce the number of transmissive components in the beam path, an alternative design with only two lenses called D003 imaging system [6] was studied (Fig. 2). It was designed without the need to provide a collimated beam at the photo diode. It features suppression of the beam walk on the photo diode and a magnification factor of 3:1. This magnification is required because in the LISA TM interferometer the nominal waist radius is 1 mm while the QPD radius is only 0.5 mm. By compressing the beam size with an imaging system, more light power can be used in detection and stray light originating from the QPD borders can be suppressed [6]. The imaging system is defined as the positions and parameters of the lenses as well as the position and the properties of the photo diode. A list of these parameters can be found in Table 1. They
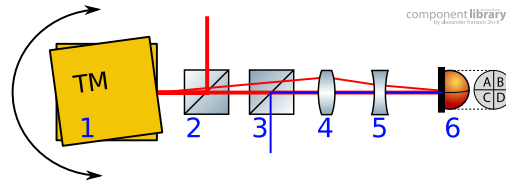
Fig. 1. Working principle of a test mass interferometer with imaging system. The measurement beam (red) is reflected at the TM (yellow) and interfered with the reference beam (blue). The TM angle is measured by using DWS [7], the longitudinal TM movement corresponds to the phase change in the interferometer. The imaging system images the point of reflection from the TM to the photo diode and therefore suppresses beam walk o the diode. All components in this sketch are labeled in order to make them easily visible in later schematics. 1 test mass, 2 polarizing beam splitter, 3 recombining beam splitter, 4 lens one, 5 lens two, 6 quadrant photo diode.

were found by numerically optimizing the lens positions for minimal TTL coupling for a large number of combinations of off-the-shelf spherical lenses.

Table 1. Specifications of the D003 imaging system. The point of rotation is assumed to be on axis at longitudinal position 0.0 mm. The QPD slit width indicates the width of the insensitive area between the QPD segments. The magnification is 3:1.

|  | Unit | Lens 1 | Lens 2 | QPD |
|---|---|---|---|---|
| Position | mm | 425.00 | 472.89 | 525.24 |
| Nominal Focal Length | mm | 60.00 | -50.00 | |
| Primary Curvature | 1/m | 31.39 | -19.80 | |
| Secondary Curvature | 1/m | 0.00 | -19.80 | |
| Center Thickness | mm | 4.00 | 1.50 | |
| Substrate Radius | mm | 11.20 | 11.20 | |
| Refractive Index | 1 | 1.51 | 1.45 | |
| QPD Diameter | mm | | | 1.00 |
| QPD Slit Width | $\mu$m | | | 20.00 |

With the help of numerical simulations (IfoCAD [8, 9]) it could be shown that this kind of imaging system should be able to reduce the TTL coupling significantly. The simulated TTL coupling with and without the D003 imaging system for a typical LISA-like TM-interferometer and a perfectly aligned system is shown in Fig. 3. The left-hand graph shows the path length change plotted over the beam angle in the scenario without imaging system, a tilt of one laser beam by a few hundred micro radian results in an unwanted longitudinal path length change in the readout of a few tens of nanometers. In contrast, the graph on the right (Fig. 3) shows the TTL coupling in the same interferometer with an additional imaging system, the amount of path length change is reduced below 0.05 nm.

## 3. Mechanisms of tilt-to-length coupling

The D003-performance simulations in the previous section assumed a perfectly aligned setup under ideal conditions. However, this does not apply to any experimental realization. Small misalignments like lateral or longitudinal positioning offsets of the lenses or variations of the focal lengths are unavoidable. Any of those imperfections are a possible source of additional TTL coupling. These need to be controlled carefully in the experiment in order to allow a
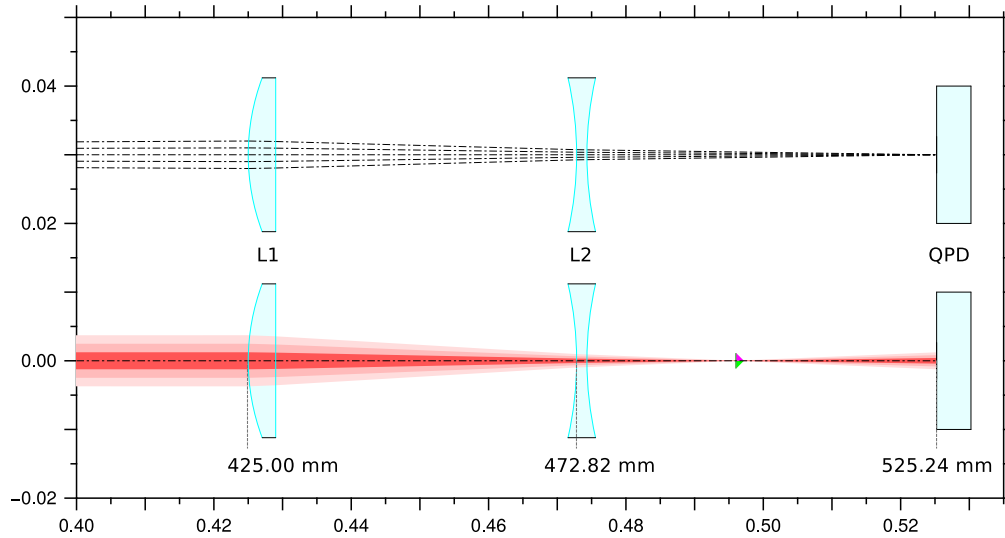
Fig. 2. D003 imaging system design. The longitudinal positions of the centers of the front surfaces of the lenses and the QPD are marked, while the point of rotation (TM) is located at position 0 mm. The first plot shows the propagation of different base rays, which start under different angles at the point of rotation and end up in the center of the QPD (demonstrating zero beam walk). The second plot is showing the propagation of a Gaussian beam. The triangle indicates the waist position. Furthermore, the magnification factor can be seen. The large 1 mm waist Gaussian beam is compressed and becomes much smaller on the QPD.
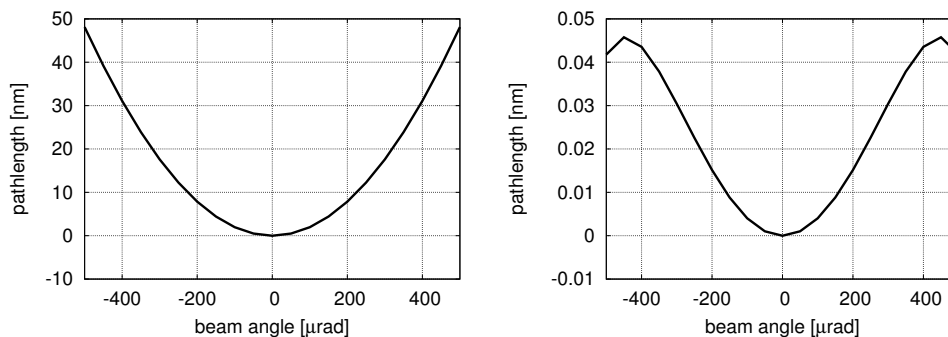


Fig. 3. Simulated TTL coupling in the LISA TM interferometer without (left) and with (right) the D003 imaging system and a perfectly aligned setup. With the help of the imaging system D003 the TTL coupling can be reduced significantly.

comparison to the simulations. In the following, the different relevant TTL coupling sources are discussed.

### 3.1.  Parasitic longitudinal movement of the tilt actuator

To realize a tilting beam in an experiment, usually a tilt-actuator is used. The main challenge is that the mirror mounted to the actuator often does not tilt around a fixed pivot in the center of the mirror's surface. The real pivot is located with an offset and might slightly move during one tilt-cycle. With a smart driver that controls fine adjusted linear combinations of three piezos, for

example, it is possible to reduce this noise source, but since the longitudinal movement couples directly in the measurement, it has to be reduced significantly below the interferometer sensitivity. To remove the TTL coupling caused by the longitudinal movement of the tilt-actuator in our setup, we measure the interference pattern with a large single element photo diode (SEPD). As shown in [10], a large SEPD is not affected by TTL coupling in the case of equal beam shapes and no lateral offset between the beams and the pivot.

### 3.2. Wavefront curvature mismatch

We use a homodyne equal arm-length Mach-Zehnder interferometer in order to match the beam parameters perfectly, to allow the SEPD to sense solely the longitudinal motion of the actuator. Otherwise, unmatched beam parameters would generate additional TTL coupling. The main reason for this is a mismatch between the wavefront curvatures of the beams in the detector plane. Figure 4 shows a qualitative explanation of the effect. A reference beam (blue wavefront) and a measurement beam (red wavefront) are interfered. The arrows symbolize the local phase difference between the two wavefronts at different positions ($\Phi_i$). The photo diode and the phase decomposition is simplified by a summation over all $\Phi_i$. The resulting total phase is shown as a green arrow. The angle of the green arrow contains the phase, while its length is related to the contrast (described in Sec. 5).

If the wavefronts and the pivot are well aligned as shown in the upper part of Fig. 4, the phase difference is equal for all $\Phi_i$. The averaged total phase will be equal to each single phase of the $\Phi_i$. By tilting two beams against each other, an additional-phase-difference will appear between the measured wavefronts. This additional-phase-difference increases with the lateral distance to the pivot. The same phase difference will appear on both sides of the pivot, but in opposite directions. By measuring the entire interference pattern, the additional-phase-differences cancel each other and the resulting total phase will stay constant (compare the angle of the two green arrows in the upper part of Fig. 4).

If the wavefront curvatures happen to be unequal (lower part of Fig. 4), the values of the $\Phi_i$ will vary, depending on the curvature mismatch. Therefore, the averaged total phase will be different from the single $\Phi_i$ phases. If the wavefronts with different curvatures are tilted they see the same additional-phase-difference which appears on both sides with different sign and increases with lateral distance. By measuring the entire interference pattern these additional-phase-differences still cancel each other, but will result in a loss of contrast in the interferometric signal. This loss of contrast as well as the additional-phase-difference depends on the lateral distance to the pivot. Therefore, a wavefront tilt will discriminate the $\Phi_i$ in the outer areas of the photo detector. For equal wavefronts this is uncritical since every point on the detector gives the same signal. But for unequal wavefronts, each point generates a different phase signal. By tilting the wavefronts, the balance between the different phases changes and thus the resulting total phase signal (the average of the $\Phi_i$) changes, too. This can be seen in the two green arrows in the bottom half of Fig. 4. The total phase in the titled scenario is shorter (loss of contrast) and has a different angle (the phase has changed).

### 3.3. Higher order Gaussian modes

Higher order Gaussian modes of odd order generate in general an asymmetric amplitude profile (see Fig. 5), which disturbs the phase readout, since the phases at the different detector positions are weighted with the product of the electric fields amplitudes. We get rid of higher order modes with the use of an optical resonator.
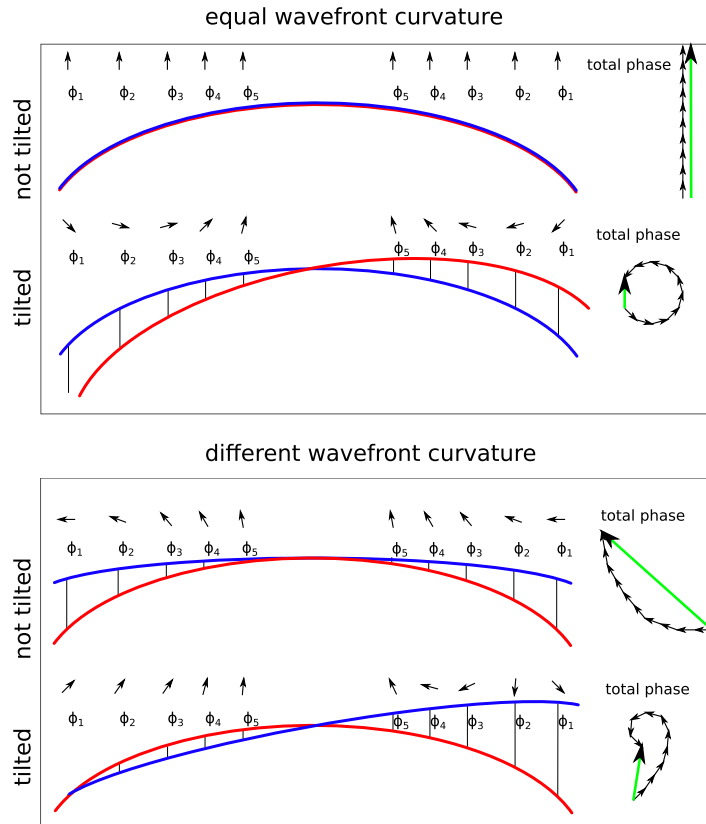
Fig. 4. Demonstrative explanation of the TTL coupling generated by a wavefront curvature mismatch. For simplicity, the electric field amplitudes are considered to be constant over the detector's surface.

## 4. Experimental setup

A schematic of the experimental setup is shown in Fig. 6. To ensure that both beams in the experiment are equal and have the same wavefront curvature at the detector (to suppress unequal beams, compare to Sec. 3.2), a homodyne equal arm-length Mach-Zehnder interferometer with only one light source is used. The path length is measured with multiple different detectors which will be described subsequently.

The optical resonator (called mode cleaner [11]) in front of the experiment produces a purely fundamental Gaussian beam to suppress higher order modes (compare to Sec. 3.3). The resonator comprises two plane mirrors and one concave mirror with a radius of curvature of 1 m. The resonator round-trip length measures 416 mm. The eigenmode has a waist radius of 370 μm located between the two plane mirrors. After the resonator a telescope magnifies the eigenmode to a waist radius of 1 mm located roughly at the tilt mirror, which is representative for LISA. The resonator was used with p-polarized light and has a finesse of 360. The cavity round-trip length can be actuated by a piezo crystal attached to the concave mirror. It is stabilized using the tilt-lock technique [12]. The control loop has a unity gain frequency of $\approx 15\,\text{kHz}$ and a phase margin of $\approx 40°$.

The tilting of the beam is performed by a commercial piezo driven tilt-actuator and an additional quadrant photo diode (QPD) is placed behind the tilt-actuator in order to monitor the
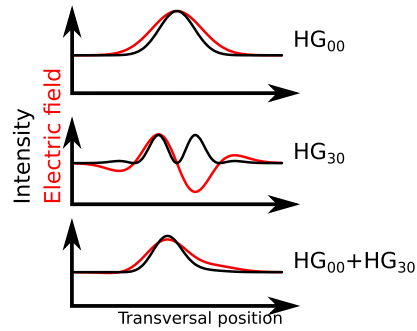
Fig. 5. A fundamental Gaussian mode is mixed with a Hermite-Gaussian 30 mode, the resulting beam is asymmetric.
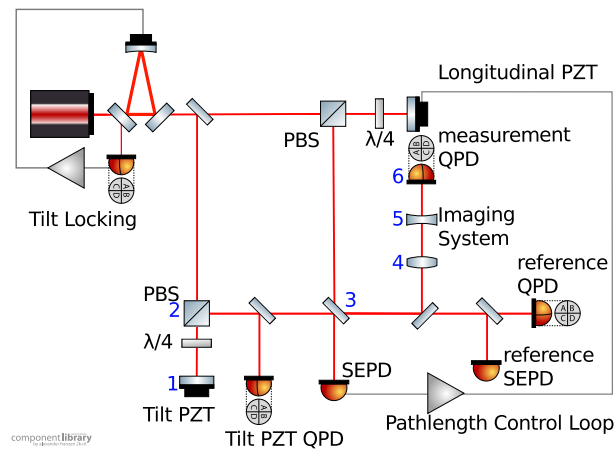


Fig. 6. Draft of the experimental setup, with: polarizing beam splitter (PBS), quarter wave-plate ($\lambda/4$), quadrant photo diode (QPD), single element photo diode (SEPD), piezo driven actuator (PZT). The key components from Fig. 1 are labeled in blue.

actual tilt angle. This tilt-QPD measures the difference of the power between its sides (differential power sensing signal - DPS) [9, 13]. By tilting the beam, its center moves over the photo diode's surface and the DPS signal varies.

To remove the TTL coupling caused by the longitudinal movement of the tilt-actuator (compare to Sec. 3.1), the interference pattern is measured with a large single element photo diode (SEPD). The SEPD will only detect the longitudinal movement of the tilt-actuator in the interference pattern. As shown in [10], a large SEPD is not affected by TTL coupling in the case of equal beams and no lateral offset between the beams and the pivot. Due to the resonator and the equal arm-length Mach-Zehnder design, this is guaranteed here.

This movement is minimized by a control loop and a linear actuator in the second arm. This control loop also ensures a stable midfringe lock. A unity gain frequency of $\approx 195\,\mathrm{Hz}$ and a phase margin of $\approx 25°$ were measured. This path length control loop uses the photo current of an SEPD as a sensor. Only if the interferometer is perfectly locked to midfringe, the SEPD power theoretically does not change with the beam angle. At any other operating point, the beam tilt couples into the power detected by the SEPD. To avoid additional coupling which appears by a mismatch between operating point and midfringe and to suppress the angular dependency of the midfringe level, the interference pattern was measured with an additional

SEPD (reference SEPD). The residual coupling, measured with this reference SEPD, was in the end subtracted from the TTL coupling, measured behind the imaging system.

Besides the reference-SEPD, a measurement-QPD measured the TTL coupling behind an imaging system and a reference-QPD measured the TTL coupling without an imaging system.

## 5. Photo diode calibration

In a homodyne interferometer a photo diode can only detect power ($P$). If the phase difference between the two beams is equal to an even multiple of $\pi$ they interfere constructively and the power is $P_{max}$. If the phase difference is equal to an uneven multiple of $\pi$ they interfere destructively and the power is $P_{min}$. By comparing the measured power to $P_{max}$ and $P_{min}$ it is possible to compute the phase relation between the two beams. The minimal and maximal power depend, besides the beam geometry and alignment, also on the beam angle. Therefore, the two power extrema have to be measured for any beam angle and every specific photo diode. In Fig. 7, $P_{min}$ and $P_{max}$ are plotted over the DPS signal of the tilt-QPD (which we use as measure for the beam angle) for the measurement-QPD, the reference-QPD and the reference-SEPD. These measurements were obtained by applying a slow sinusoidal waveform to the tilt piezo and a fast sinusoidal waveform to the longitudinal piezo while monitoring the power on all diodes.
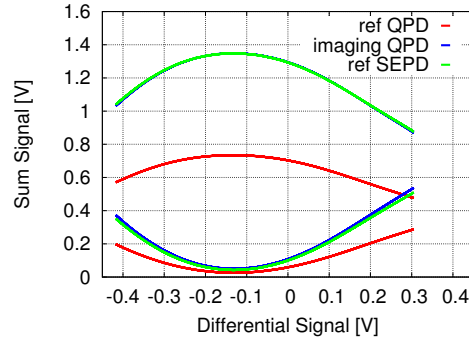


Fig. 7. Angle dependent maximal and minimal power on the different photo diodes (sum signal∝power, differential signal∝DPS).

The power $P$ on a QPD can be expressed as a function of the phase-difference $\Delta\varphi$ between the two beams

$$P := \bar{P}\left[1 + c\,\sin(\Delta\varphi)\right] . \tag{1}$$

Here, the contrast $c$ is

$$c := \frac{P_{max} - P_{min}}{P_{max} + P_{min}}, \tag{2}$$

and the mean power $\bar{P}$ is

$$\bar{P} := \frac{P_{max} + P_{min}}{2} . \tag{3}$$

Therefore, the phase-difference becomes

$$\Delta\varphi := \arcsin\left[\frac{2P - (P_{max} + P_{min})}{P_{max} - P_{min}}\right], \tag{4}$$

and the related longitudinal path length signal (LPS) gets

$$s_{LPS} := \frac{\lambda}{2\pi}\,\Delta\varphi . \tag{5}$$

Since $P_\text{max}$ and $P_\text{min}$ are a function of the beam angle, the LPS signal depends on the beam power and the beam angle, too.

## 6. Coherent filtering

Often, high precision experiments are built on highly temperature stable glass baseplates and are operated in vacuum to suppress the influence of pressure, air fluctuations, and temperature (e.g. the optical bench of LISA pathfinder [4]). The present experiment is built as a table top experiment on a steel breadboard and is operated in air.

To suppress the mentioned noise sources anyway, a filter technique that we call coherent filtering is used. The idea is to apply a modulation to the tilt actuator, measure many cycles of the resulting interferometric signals and perform a fast Fourier transformation (FFT). Any signal frequency which is unequal to the modulation frequency or higher harmonics can not be caused by the actuator and therefore must be noise. By computing the inverse transformation of only those bins, which correspond to the modulation frequency and higher harmonics, only the beam tilt dependent parts of the signals are left.

In order to use coherent filtering, some technical conditions have to be fulfilled. The sampling frequency of the signal readout system must be an exact integer multiple of the tilt piezos modulation frequency. Therefore, a strict phase-lock between the tilt piezos function generator and the signal readout is required. Furthermore, the measurement length for the coherent filtering must be an integer multiple of the piezos modulation period.

In the presented experiment the sampling frequency is 20 kHz, the tilt piezos modulation frequency is 0.2 Hz and the measurement time is 90 s.

## 7. Post-processing

In a measurement, the tilt actuator is tilted sinusoidally. The power signal of the reference-QPD, the measurement-QPD, the reference-SEPD and the DPS signal of the tilt-QPD are measured over several tilt cycles. All signals are coherently filtered. The different power signals are transformed to the corresponding LPS signals via the calibration of the different photo diodes. The TM-tilt DPS signal is transformed to the real beam angle via the tilt actuator-QPD calibration. Afterwards, the LPS signal of the reference-SEPD is subtracted from both, the measurement-QPD and the reference-QPD. In the end, the two QPD signals are plotted against the beam angle and the related signal slopes are computed.

## 8. Results

Figure 8 shows the LPS signal and its slope as measured in the experiment for the measurement-QPD with imaging system and the reference-QPD without imaging system, compared to numerical simulations which were performed with IfoCAD [8,9]. The measured and the simulated TTL coupling on the reference-QPD match very well. Both, amount and shape of the TTL coupling appear similar.

To provide a proper comparison between simulation and measurement the residual misalignment in the experiment has to be considered in the simulation. It is impossible to determine which parameter is misaligned, since many of the possible misalignments produce TTL coupling of the same shape and we can not measure all misalignment parameters with the required precision. Therefore, the set of misalignment parameters was chosen, which can explain the measured coupling with the most simple combination of misalignments. The misaligned parameter is a transversal misalignment of the first lens of 0.7 μm. This misalignment was applied to the simulation. The assumed combination of misaligned parameters is one possibility to explain the measured TTL coupling. Nevertheless, it can be concluded that within the ex-

perimental alignment accuracy, the measured performance of the imaging system matches the simulated results.
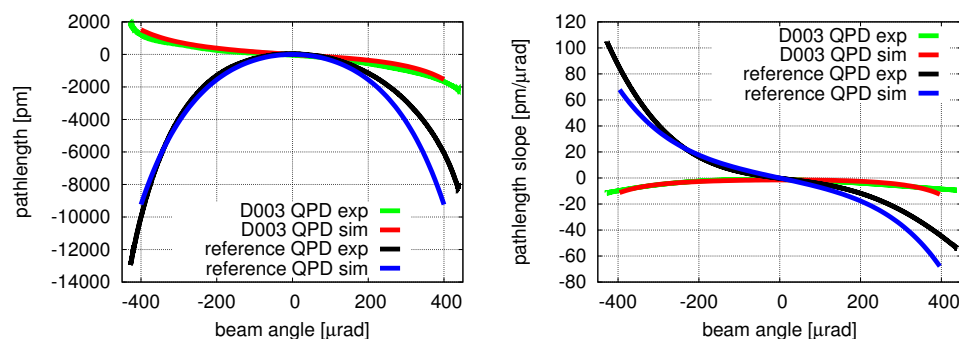


Fig. 8. LPS signals and slope of the measurement-QPD (behind the D003 imaging system) and reference-QPD compared to a numerical simulation.

## 9. Discussion

In order to understand and manage a noise budged for a complex system like LISA it is of great importance to know and understand the single noise sources in detail. In the setup shown above the effect of an isolated imaging system was observed and studied.

Without imaging system, the measured TTL coupling rises up to 100 µm/rad. By using the imaging system, the TTL coupling could be reduced in the complete angular range below ±15 µm/rad. Moreover, in the small angular tilt range of ±100 µrad, the slope could even be reduced to less than 2 µm/rad. The imaging system design D003 is able to suppress the TTL coupling significantly and behaves as expected from the numerical simulations. The residual coupling which is higher than the theoretical possible performance can be explained with a residual misalignment. Therefore, this type of two lens imaging system is a possible solution to suppress TTL coupling.

With the knowledge of the performance of an isolated imaging system further investigations become possible that will show the overall performance of individual interferometric designs that comprise imaging systems.

The shown performance of an imaging system was achieved in a homodyne Mach-Zehnder interferometer with equal beams without higher-order modes. The baseline concept for LISA foresees heterodyne interferometry instead of a homodyne readout [3, Sec. 4.1.1]. However, the TTL coupling should not depend on the readout scheme. Unequal beams and the presence of higher-order modes affect the TTL coupling. The coupling strongly depends on the specific beam parameter mismatch and higher-order mode content and hence the specific mission design. In a future publication we plan to report on a different experiment involving unequal beams and possibly higher-order modes. In this experiment we have used a large SEPD as reference. As was shown in [10] this scheme is only valid for equal beams without higher-order modes.